Electronic Supplementary Material (ESI) for Chemical Communications.

The Influence of Exogenous Amines on the Electrochemical CO_2 Reduction Activity of a Cobalt-Pyridyldiimine Catalyst

Piyush Kumar Verma[a] and Charles C. L. McCrory[a,b,*]

[a] Department of Chemistry, University of Michigan, Ann Arbor, Michigan, 48109-1055, United States.

[b] Macromolecular Science and Engineering Program, University of Michigan, Ann Arbor, Michigan, 48109-1055, United States.

*Corresponding author: Charles C. L. McCrory: cmccrory@umich.edu

1. Experimental Information

1.1. Materials and General Methods

Unless otherwise noted, all commercial chemicals were used as received without further purification. Acetone (ACS grade), aniline (ACS grade), hexanes (ACS grade), dichloromethane (ACS grade), and diethyl ether (ACS grade) were purchased from Fisher Scientific. Ethanol (EtOH, 200 proof, anhydrous) was purchased from Decon Laboratories, Inc. Acetonitrile (MeCN, HPLC plus, ≥99.9%), Isopropanol (ACS grade, ≥99.5%) and dimethylammonium dimethylcarbamate (DMA-CO_2, ratio of CO_2-Dimethylamine <2:1) were purchased from Sigma Aldrich. The typical water concentration in commercial MeCN has been previously measured to be ~0.04-0.14 M.[S1-3] Tetrabutylammonium hexafluorophosphate (nBu_4NPF_6, > 98.0%) was purchased from TCI America and recrystallized from ethanol before use. Cobalt bromide (99%), hydrogen bromide aqueous solution (ACS reagent, 48%), Ferrocene (98.0%) and silver nitrate (ACS reagent, Assay 100.2 %) was purchased from Sigma Aldrich. 1,1'-bis(diphenylphosphino)-ferrocene-palladium(II)dichloride ($Pd(dppf)Cl_2$, 97.0%), cesium fluoride (CsF, 99.0%), 4-bromopyridine hydrochloride (99%) and pyridine-4-boronic acid hydrate (96%) was purchased from Oakwood Chemical. 3,3'-diaminodipropylamine (>98%) was purchased from TCI America. Water used in this study was purified to 18.2 MΩ cm resistivity using a Thermo Scientific Barnstead GenPure UV-TOC/UF xCAD-plus water purification system. Nitrogen (N_2) was boil-off gas from a liquid nitrogen source. Carbon dioxide (CO_2, Bone dry grade, >99.8%) and Argon (Ar, pre-purified grade, 99.998%) were purchased from Cryogenic Gases.

All amines studied were passed through a silica plug before use. *N*-butylamine (NBA, 99%) was purchased from Acros Organics. Diisopropylamine (DIA, 99.5%), dimethylamine (DMA, 40 wt% in water), monoethanolamine (MEA, 99%), and *N,N,N*-trimethyl-1,3-propanediamine (TMPDA, 96%) were purchased from Sigma-Aldrich.

NMR spectra were recorded on Varian 600 MHz cryoprobe NMR spectrometer and chemical shifts are reported in ppm relative to trace of non-deuterated solvents present. UV-Visible (UV/Vis) spectra were recorded on Lambda 265 PDA UV/Vis Spectrophotometer with a photodiode array detector (PerkinElmer). The IR spectrum was recorded on Thermo Scientific iS50 FT-IR instrument. Scanning Electron Microscopy/Energy Dispersive X-ray spectroscopy (SEM-EDS) measurements were performed on JEOL JSM-7800FLV Scanning Electron Microscope and Oxford XMaxN 80mm² silicon-drift energy-dispersive X-ray spectrometer respectively. The data was processed on Oxford Aztec v3.3 EDS acquisition and processing software.

1.2 Synthesis of [Co(PDI-Py)Br$_2$]Br.

The complex [Co(PDI-Py)Br$_2$]Br was synthesized according to the reported literature procedure as follows.[S4]

Synthesis of 4-Bromo-2,6-diacetylpyridine (compound 1). 4-Bromopyridine hydrochloride (2.92 g, 15.0 mmol) was basified by Na_2CO_3 aqueous solution to pH 10 followed by its extraction by dichloromethane (DCM, 3 × 40 mL). 4-Bromopyridine dissolved in this DCM solution was extracted by 0.4 M H_2SO_4 solution in water (4 × 25 ml). The aqueous solution was transferred to a two neck round bottom flask and bubbled through N_2 for 15 minutes. Under N_2 flow, pyruvic acid (2.32 g, 1.83 mL, 26.4 mmol), $AgNO_3$ solution (0.123g, 0.726 mmol in 0.3 mL H_2O) and $(NH_4)_2S_2O_8$ (9.10 g, 40.0 mmol) was added into the solution slowly. The solution was stirred at the room temperature for 24 h. The mixture was filtered through a celite frit, and the solid was further rinsed with DCM. This filtrate mixture was extracted by DCM (3 × 40 mL). The combined DCM fraction was dried by anhydrous $MgSO_4$ and evaporated under reduced pressure to get oily residue. This oily residue was further purified via column chromatography (silica gel, hexane/ethylacetate, 4/1). Compound 1 (0.85 g, yield: 23%) was obtained as a white solid. ^{1}H NMR ($CDCl_3$-*d*, 600 MHz, Figure S1): δ (ppm) 8.3 (2H, s, Py-H), δ 2.8 (6H, s, CH_3).

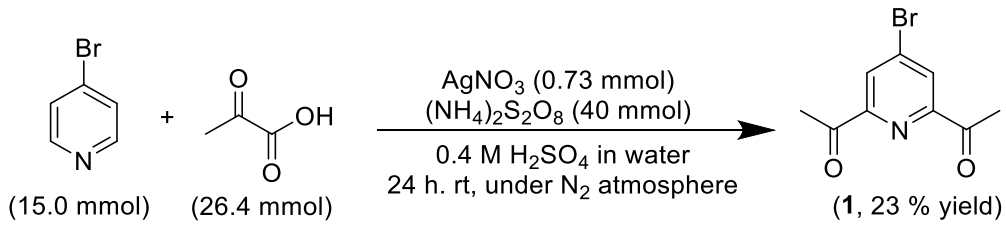

Scheme S1. Synthetic route for 4-Bromo-2,6-diacetylpyridine.

Synthesis of 4-Pyridyl-2,6-diacetylpyridine. The compound 1 (361 mg, 1.5 mmol) and 4-pyridylboronic acid (184 mg, 1.5 mmol) were dissolved in 20 mL of 1,4-dioxane/H_2O mixture (16 ml/4 ml), and bubbled by N_2 for 30 minutes. To this reaction mixture, CsF (701 mg, 4.63 mmol) and Pd(dppf)Cl_2 (33.8 mg, 0.046 mmol) was added under N_2 flow and heated at 90 °C for 24 h. Upon cooling, the reaction was quenched by addition of 100 mL of saturated NH_4Cl aqueous solution. The mixture was extracted by EtOAc (3 × 50 mL) dried over $MgSO_4$. The solvent was removed under reduced pressure to get off white solid residue. The residue was further purified by column chromatography (silica gel, DCM/EtOAc, 2/1) to get white solid (280 mg, 78%). ^{1}H NMR ($CDCl_3$-*d*, 600 MHz, δ (ppm) Figure S2): δ 8.8 (2H, d, Py-H), δ 8.5 (2H, s, Py-H), δ 7.7 (2H, d, Py-H), δ 2.8 (6H, s, CH_3).

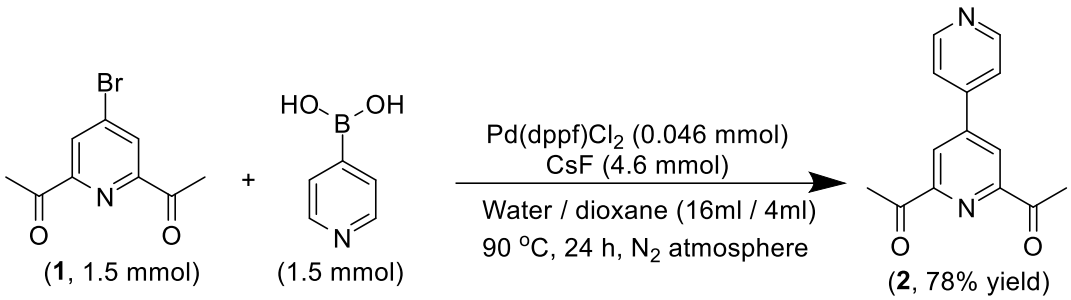

Scheme S2. Synthetic route for 4-Pyridyl-2,6-diacetylpyridine.

Synthesis of [Co(PDI-Py)Br₂]Br. To the stirring solution of 4-Pyridyl-2,6-diacetylpyridine (288 mg, 1.2 mmol) in 10.0 mL of ethanol, homogeneously dissolved solution of $CoBr_2$ (262.5 mg, 1.2 mmol) in ethanol solution was added under N_2. 3,3′-diaminodipropylamine (167.2 µL, 1.2 mmol) was added to the reaction mixture dropwise. The mixture was stirred at 55 °C for 24 h. The resulted dark purple precipitate of Co(PDI-Py)Br_2 was collected by filtration and washed with cold ethanol. This Precipitate was then suspended in 15 ml of ethanol followed by the addition of 1.5 equiv HBr (45-47 wt% in water) and stirred overnight (14 h) in air, resulting in the green solid compound [Co(PDI-Py)]Br_3. The product was collected and washed with cold ethanol to give green solid powder (370 mg, 47% yield). ^{1}H NMR (DMSO-*d6*, 600 MHz, δ (ppm), Figure S3): δ 9.1−9.0 (4H, s, s, Py*H*), δ 8.4 (2H, s, Py*H*), δ 6.7 (H, t, −CH_2N*H*CH_2−), δ 4.2 (2H, d,−*CH_2*NHCH_2−), δ 3.6 (2H, t, −C=N−*CH_2*−), δ 3.3−3.2 (4H, m, −CH_2*CH_2*CH_2− and −CH_2NH*CH_2*−), δ 3.1 (6H, s, CH_3), δ 2.3 (2H, m, −CH_2*CH_2*CH_2−), δ 2.1 (2H, m, −C=N−C*H_2*−).

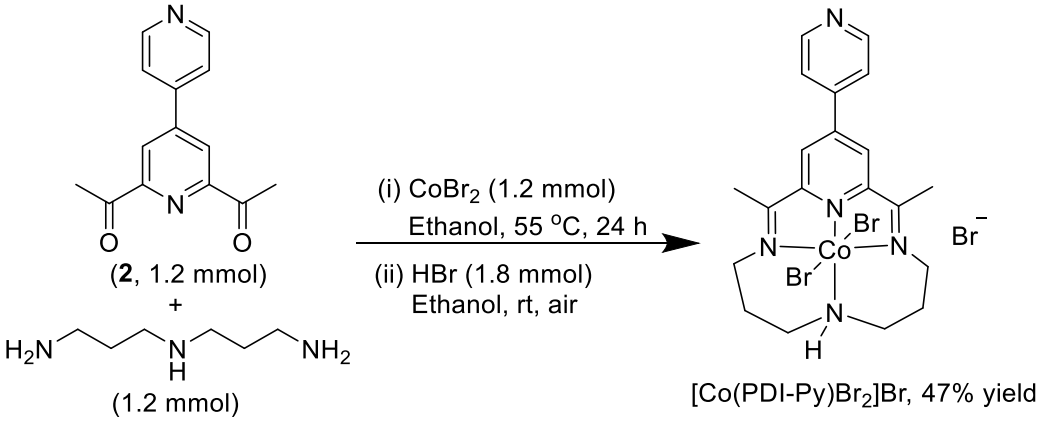

Scheme S3. Synthetic route for [Co(PDI-Py)Br_2]Br.

1.3. Electrochemical Methods and Product Analysis

Electrochemical measurements were conducted using a Bio-Logic SP-200 potentiostat/galvanostat. Data was collected and processed using the Bio-Logic EC-Lab v11.50 software package.

***Cyclic Voltammetry (CV)*:** Cyclic voltammograms were collected under either Ar or CO_2 atmosphere in quiescent solution at room temperature. The working electrode was a 0.071 cm^2 glassy carbon disk (CH instruments), the auxiliary electrode was a carbon rod (99.9%, Strem Chemicals), and the reference electrode was a $Ag/AgNO_3$(1.00 mM in MeCN with 0.100 M $n$$Bu_4NPF_6$) non-aqueous reference electrode separated from the electrolyte by a coral-por frit (BASi Inc). Typical CV experiments were conducted in electrolyte solutions containing 0.3 mM [Co(PDI-Py)], 0.1 M $n$$Bu_4NPF_6$, and 11 M H_2O in MeCN. For experiments with added amines, the specified amine was added directly to the electrolyte solution. The electrolyte was sparged with either Ar or CO_2 as indicated for ~20 min before conducting CVs. To avoid electrolyte evaporation, all gases were saturated with MeCN before use by first bubbling them through a gas-washing bottle filled with MeCN. The uncompensated solution resistance (Ru ≈ 150 Ω) in the cell was measured using a single-point impedance measurement at 100 kHz with a 20 mV amplitude about the open-circuit potential before each set of measurements. CVs were automatically corrected for iR drop at 85% through positive feedback using the Bio-Logic EC-Lab software. The typical scan rate for CVs was 0.050 V s^{-1} unless otherwise noted. Before each experiment, the working electrode was manually polished on 600-grit SiC polishing paper (Buehler, Ltd.) and sonicated for 5 min in *i*-PrOH.

Controlled-Potential Electrolysis: CPE were conducted at room temperature in a custom, gas-tight, two-compartment H-cell described in previous reports. [S4-6] The working electrode was a glassy carbon plate (2.5 cm x 1.6 cm x 0.1 cm, Sigradur G grade, HTW Hochtemperatur-Werkstoff GmbH). The non-aqueous reference electrode $Ag/AgNO_3$ was composed of Ag wire (Surepure Chemetals, Purity: 99.999% / 5N Pure) dipped in $AgNO_3$ solution (1.00 mM $AgNO_3$ in MeCN with 0.100 M $n$$Bu_4NPF_6$) and the electrode was separated from the electrolyte by a coralpor frit (BASi Inc). The counter electrode was a Nichrome wire (0.2595 Ω ft^{-1}, Arcor Electronics).

One compartment held the working and reference electrode submerged in 20 mL of electrolyte solution containing 0.3 mM [Co(PDI-Py)Br_2]Br, 0.1 M $n$$Bu_4NPF_6$, and 11 M H_2O in MeCN. The working electrode was positioned such that half of the electrode was submerged in the electrolyte solution. The second compartment held the auxiliary electrode submerged in 15 mL of electrolyte solution containing 0.1 M $n$$Bu_4NPF_6$, 11 M H_2O, and 5 mM Fc. The two compartments were separated by a fine-porosity glass frit. For experiments with added amines, the specified amine was added directly to the electrolyte in the working electrode chamber. Before each CPE, the electrolyte in both chambers was sparged for ~30 min with CO_2. To avoid electrolyte evaporation, CO_2 was saturated with MeCN before use by first bubbling them through a gas-washing bottle filled with MeCN. The total volume of the H-cell was determined by measuring the mass of H_2O necessary to completely fill the cell while it was in fully assembled condition with the working, counter, and reference electrodes present. The headspace volume of the cell was calculated by subtracting the electrolyte solution volume 35.00 mL from the total cell volume.

CPE experiments were conducted at ~1 atm total pressure in stirred solutions using a stir bar at 250 rpm. CPEs were conducted without *i*R compensation for solution resistance (*R*u ≈ 50 Ω). All reported potentials for CPE experiments are the applied potentials. After each electrolysis, 8 mL

aliquots of the headspace of the H-cell were collected using a gas-tight Pressure-Lok syringe (10 mL, Valco VICI Precision Sampling, Inc.), and injected into the 3.00 mL sample loop in a GC system to determine CO and H_2 concentrations. Selected post-electrolysis solutions were also analyzed using ^{1}H NMR to determine the concentrations of any possible solution-phase products such as HCOOH, but no solution-phase products were detected. All the working electrodes examined by SEM-EDS for post-electrolysis analysis (at 15 kV accelerating voltage) and were not rinsed as per the established practices.[S5] For each electrode, SEM-EDS measurements were conducted at 9 random sites on the electrode surface, and the values were then averaged to give the Co weight % for that specific electrode. The reported errors are standard deviations of all EDS measurements for a particular electrolysis experiment.

Faradaic Efficiency (FE) Calculations: Faradaic Efficiency (FE) is equivalent to the % yield of each product formed during a Faradaic process. It was calculated by dividing the moles of each product by the moles of electrons passed during the CPE, according to the following equation:

$$FE = \frac{\frac{head\ space\ volume}{molar\ volume\ of\ gas} \times C \times n \times F}{Q}\ \%$$

Here, the *molar volume of gas* is 24.5 L mol^{-1} at 25°C and 1 atm pressure, C is the volume % of gas (CO or H_2) measured in the headspace after the CPE, $n = 2$ is the number of electrons passed per reaction to produce CO or H_2, $F = 96485$ C mol^{-1} is Faraday's constant, and Q is the amount of charge passed during the CPE measurement.

1.4. UV-Vis Experiments.

Samples for UV-Vis experiments were prepared by first making a stock solution of 0.3 mM [Co(PDI-Py)Br$_2$], 0.1 M of *n*Bu$_4$NPF$_6$ and 11 M H_2O in MeCN.

Experiment (a): To 1 mL of the stock solution, 2 ml of MeCN was added. The resulting dilute solution was sparged with N_2 for 20 min prior to collecting a UV-Vis spectrum.

Experiment (b): The solution in Experiment (a) was sparged with CO_2 for 10 min and a UV-Vis spectrum was recorded.

Experiment (c): 0.02 M NBA was added to 1 mL of the stock solution. The stock solution was sparged with N_2 for 20 min, and then 2 mL of N_2-sparged MeCN was added. A UV-Vis spectrum of the resulting dilute solution was recorded.

Experiment (d): The solution in Experiment (c) was sparged with CO_2 for 10 min and a UV-Vis spectrum was recorded.

2. Supplementary Figures and Tables

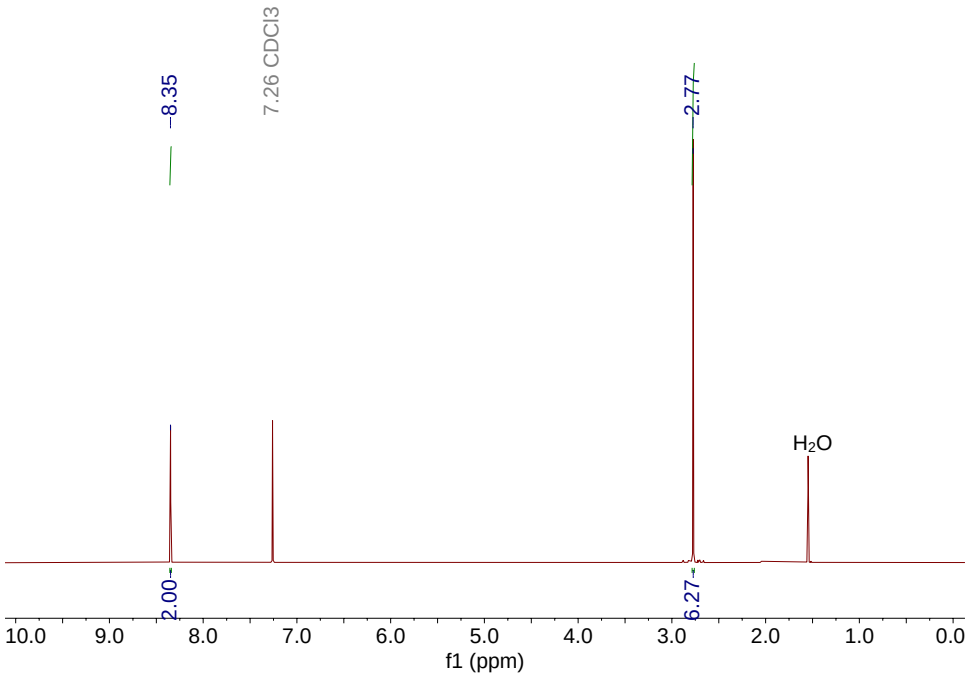

Figure S1. ^{1}H NMR spectrum of 4-bromo-2,6-diacetylpyridine in $CDCl_3$ (δ 7.26 solvent residual peak, δ 1.57 water peak).

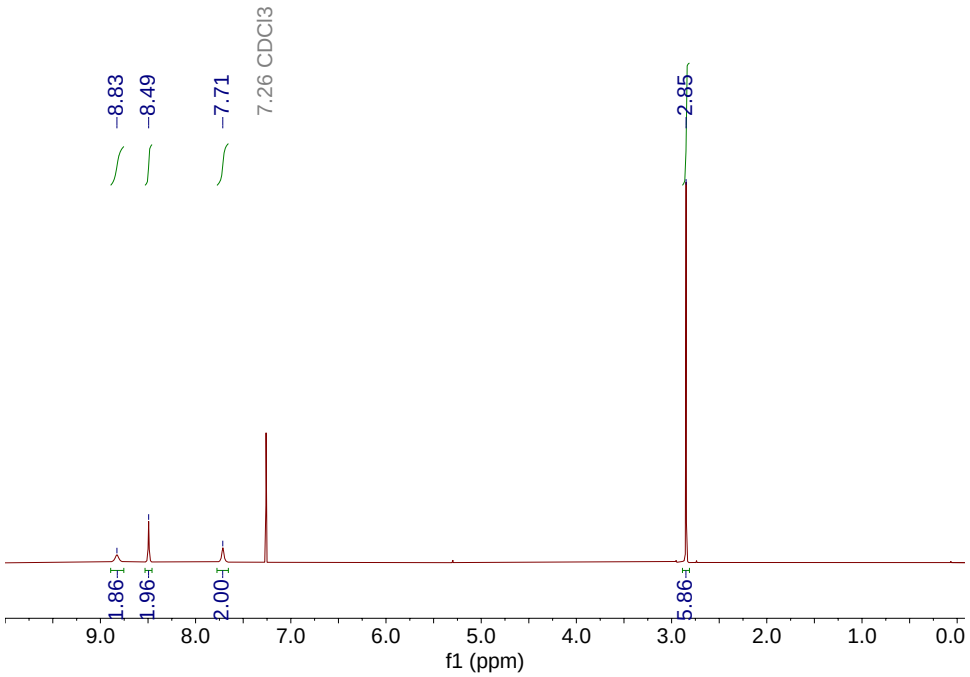

Figure S2. ^{1}H NMR spectrum of 4-pyridyl-2,6-diacetylpyridine in $CDCl_3$ (δ 7.26 solvent residual peak).

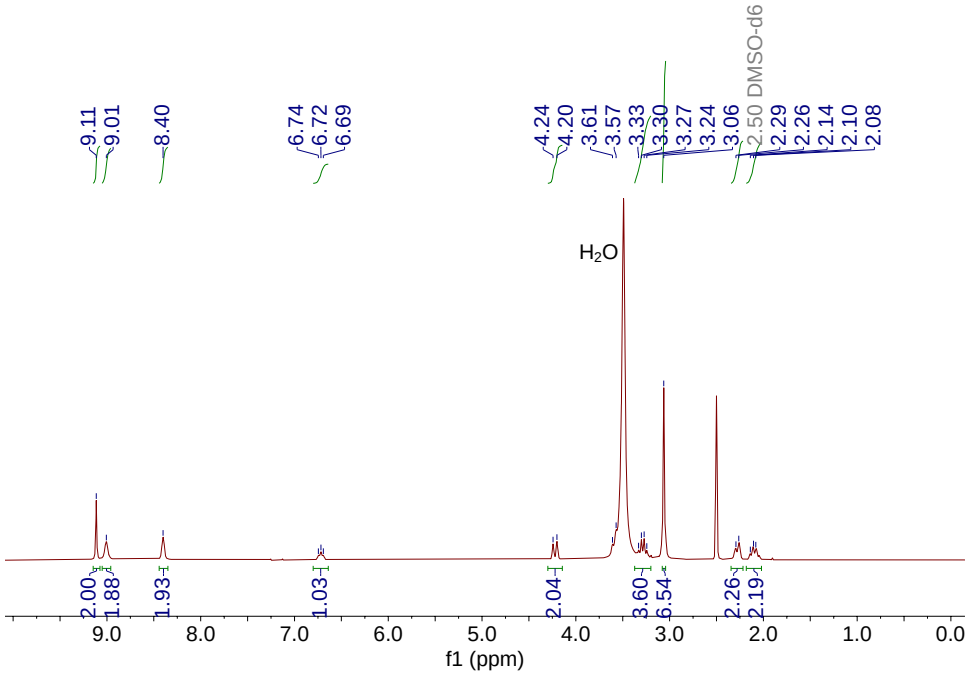

Figure S3. ^{1}H NMR spectrum of [Co(PDI-Py)Br$_2$]Br in DMSO-*d6* (δ 2.5 solvent residual peak, δ 3.3 H_2O peak).

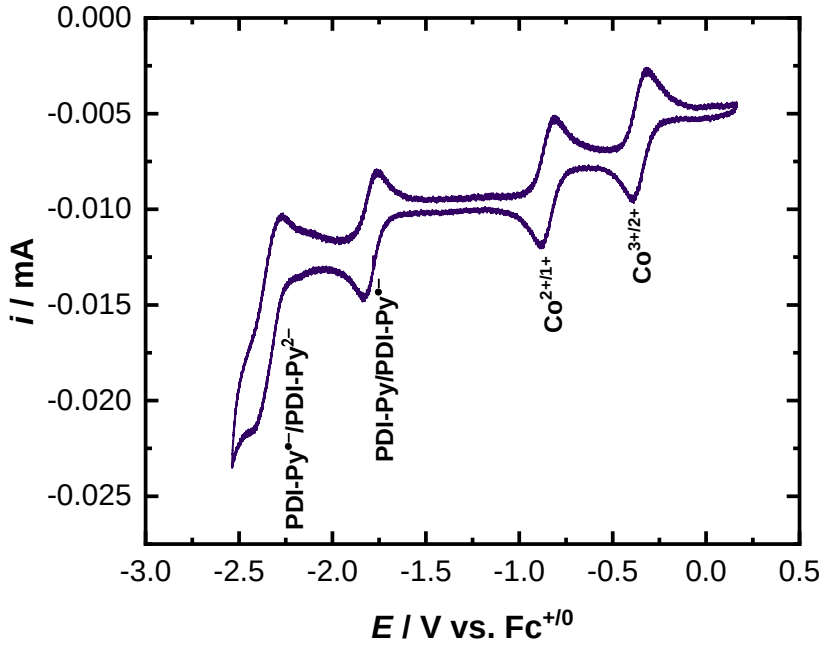

Figure S4. Representative CV of 0.3 mM [Co(PDI-Py)] in Ar-sparged MeCN with 0.1 M *n*Bu_4NPF_6 at a scan rate of 0.05 V/s.

Table S1: $E_{1/2}$ values of the redox couples for [Co(PDI-Py)] in Ar-sparged MeCN with 0.1 M *n*Bu_4PF_6.

Complex	$Co^{3+/2+}$ / V vs $Fc^{+/0}$	$Co^{2+/+}$ / V vs $Fc^{+/0}$	PDI-Py/PDI-$Py^{\bullet-}$ / V vs $Fc^{+/0}$	PDI-$Py^{\bullet-}$/PDI-Py^{2-} / V vs. $Fc^{+/0}$
[Co(PDI-Py)]	0.36	0.85	1.80	2.36

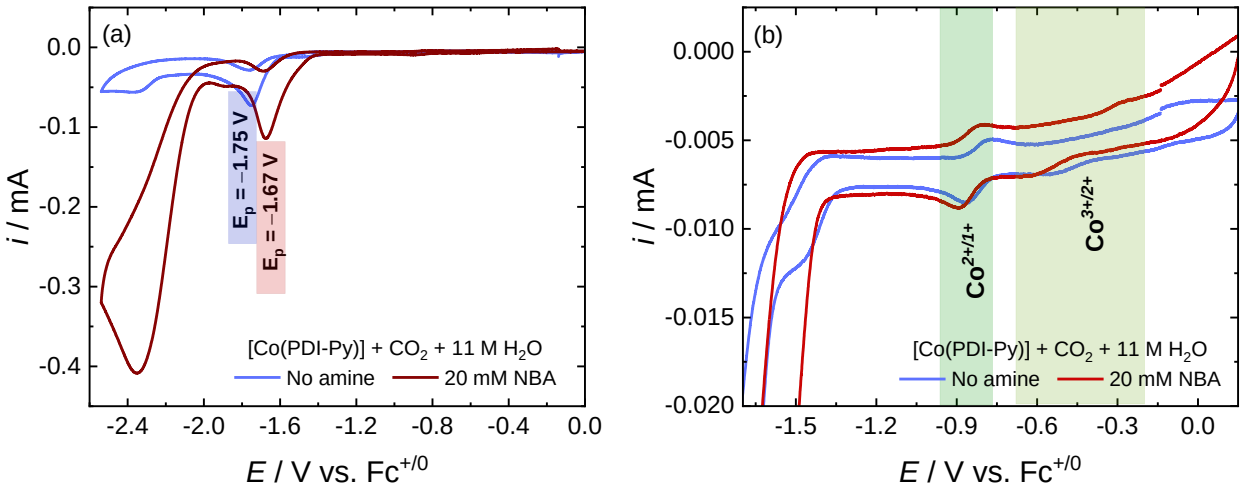

Figure S5. (a) Representative CVs of 0.3 mM [Co(PDI-Py)] in CO_2-sparged MeCN with 0.1 M nBu$_4$NPF$_6$ and 11 M H_2O at a scan rate of 50 mV/s with and without 20.0 mM NBA; (b) zoomed-in view of the $Co^{3+/2+}$ and $Co^{2+/+}$ region.

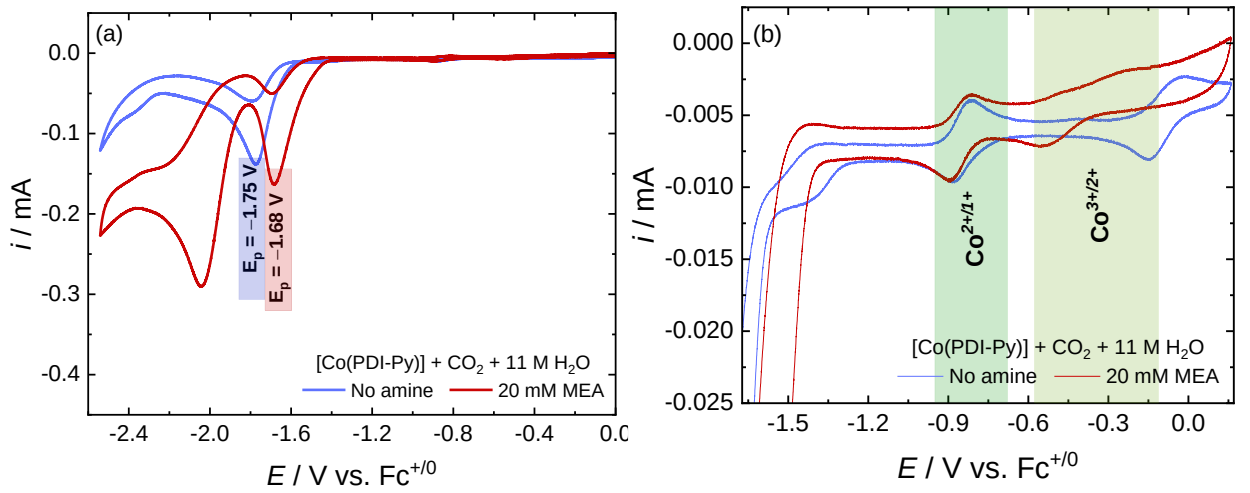

Figure S6. (a) Representative CVs of 0.3 mM [Co(PDI-Py)] in CO_2-sparged MeCN with 0.1 M nBu$_4$NPF$_6$ and 11 M H_2O at a scan rate of 50 mV/s with and without 20.0 mM MEA; (b) zoomed-in view of the $Co^{3+/2+}$ and $Co^{2+/+}$ region.

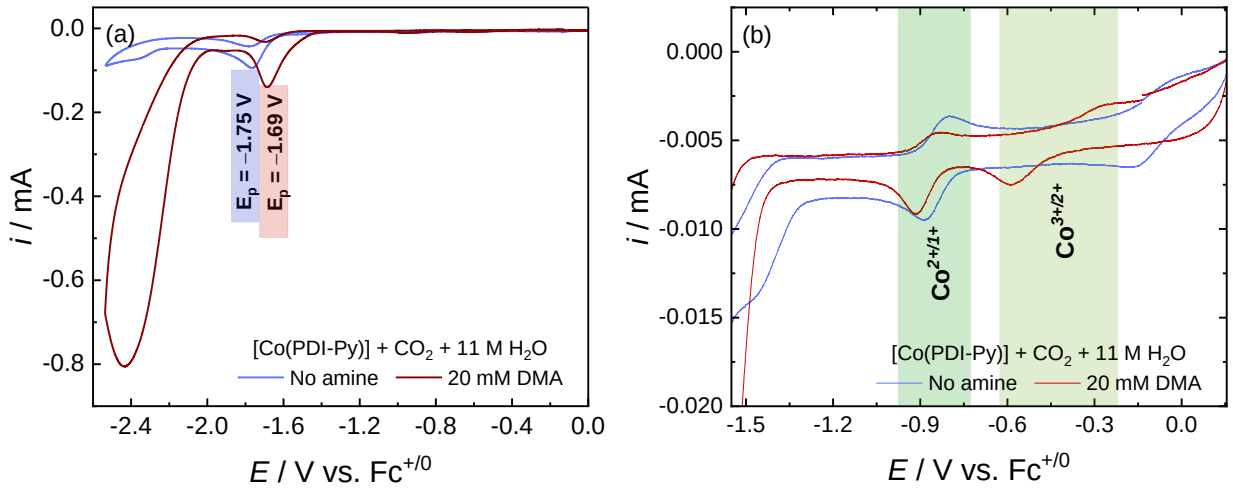

Figure S7. (a) Representative CVs of 0.3 mM [Co(PDI-Py)] in CO_2-sparged MeCN with 0.1 M nBu$_4$NPF$_6$ and 11 M H_2O at a scan rate of 50 mV/s with and without 20.0 mM DMA; (b) zoomed-in view of the $Co^{3+/2+}$ and $Co^{2+/+}$ region.

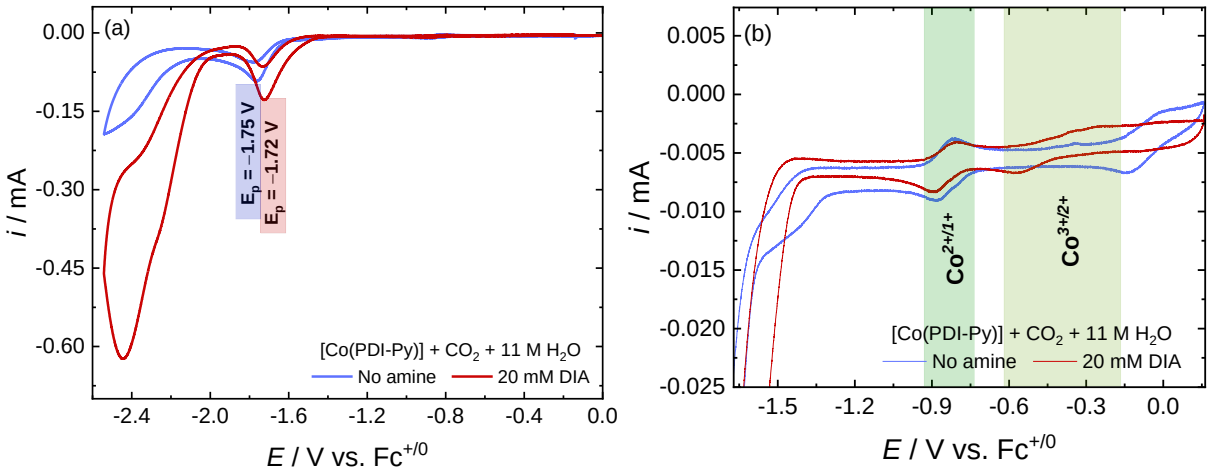

Figure S8. (a) Representative CVs of 0.3 mM [Co(PDI-Py)] in CO_2-sparged MeCN with 0.1 M nBu$_4$NPF$_6$ and 11 M H_2O at a scan rate of 50 mV/s with and without 20.0 mM DIA; (b) zoomed-in view of the $Co^{3+/2+}$ and $Co^{2+/+}$ region.

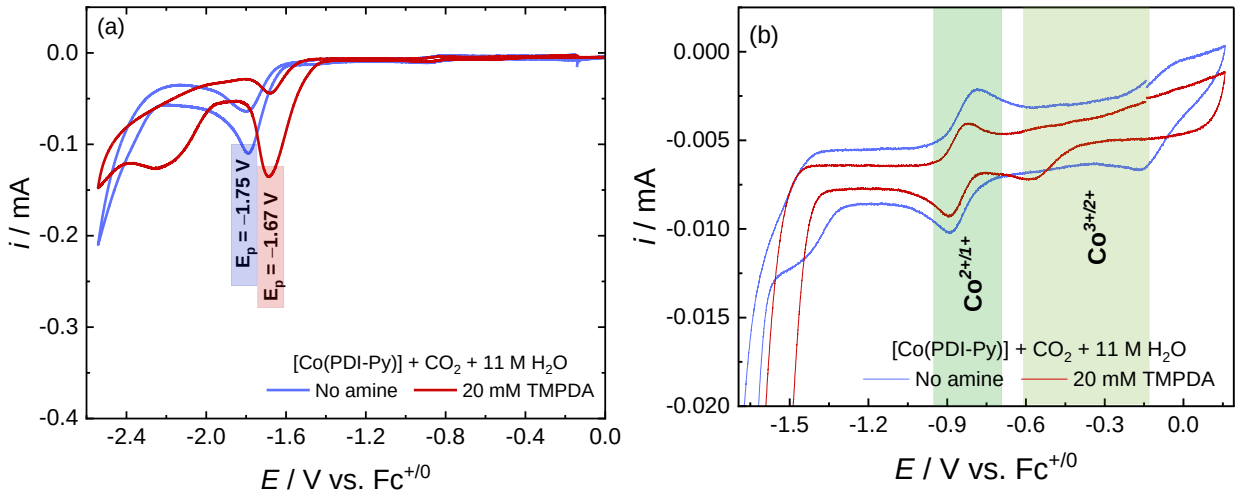

Figure S9. (a) Representative CVs of 0.3 mM [Co(PDI-Py)] in CO_2-sparged MeCN with 0.1 M nBu$_4$NPF$_6$ and 11 M H_2O at a scan rate of 50 mV/s with and without 20.0 mM TMPDA; (b) zoomed-in view of the $Co^{3+/2+}$ and $Co^{2+/+}$ region.

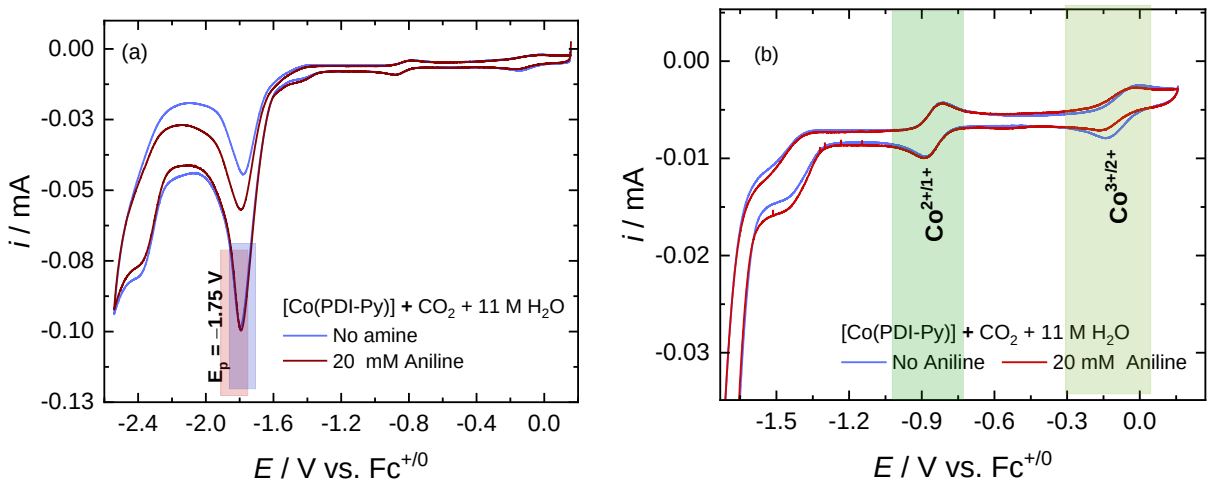

Figure S10. (a) Representative CVs of 0.3 mM [Co(PDI-Py)] in CO_2-sparged MeCN with 0.1 M nBu$_4$NPF$_6$ and 11 M H_2O at a scan rate of 50 mV/s with and without 20.0 mM aniline; (b) zoomed-in view of the $Co^{3+/2+}$ and $Co^{2+/+}$ region. Adding aniline did not result in a shift in the $Co^{3+/2+}$ or $Co^{2+/+}$ redox couples, a shift in the catalytic onset potential, or a significant increase in the magnitude of the catalytic peak current.

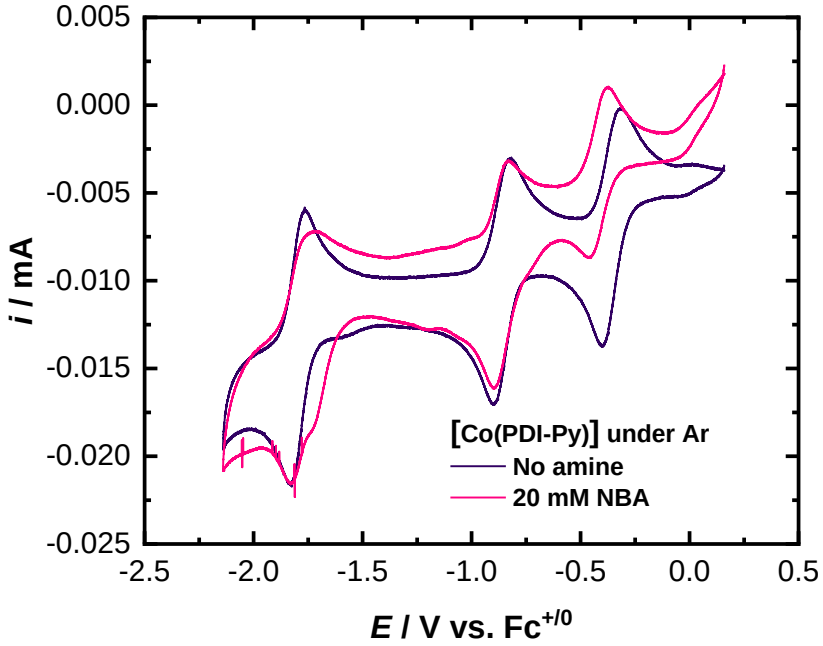

Figure S11. Representative CVs of 0.3 mM [Co(PDI-Py)] in Ar-sparged MeCN with 0.1 M nBu$_4$NPF$_6$ at a scan rate of 0.05 V/s with and without 20.0 mM NBA.

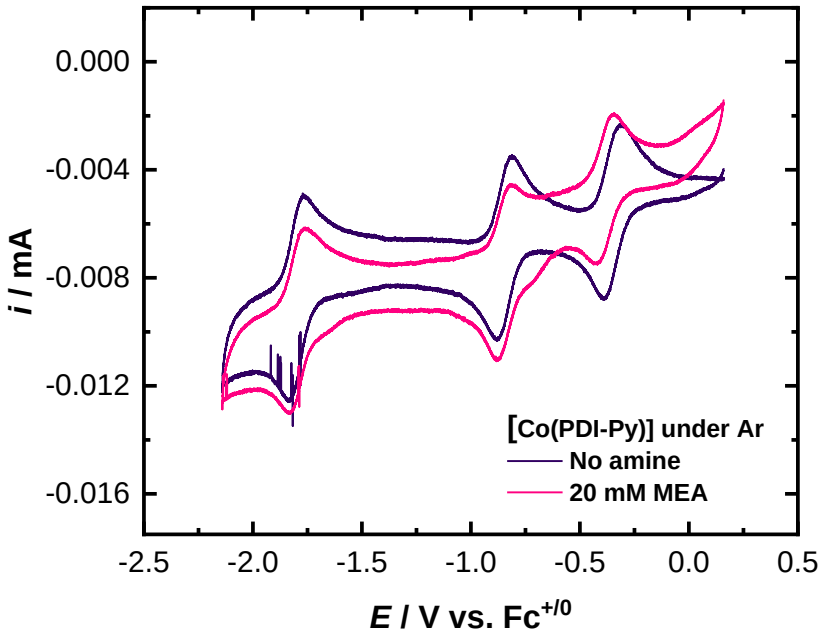

Figure S12. Representative CVs of 0.3 mM [Co(PDI-Py)] in Ar-sparged MeCN with 0.1 M nBu$_4$NPF$_6$ at a scan rate of 0.05 V/s with and without 20.0 mM MEA.

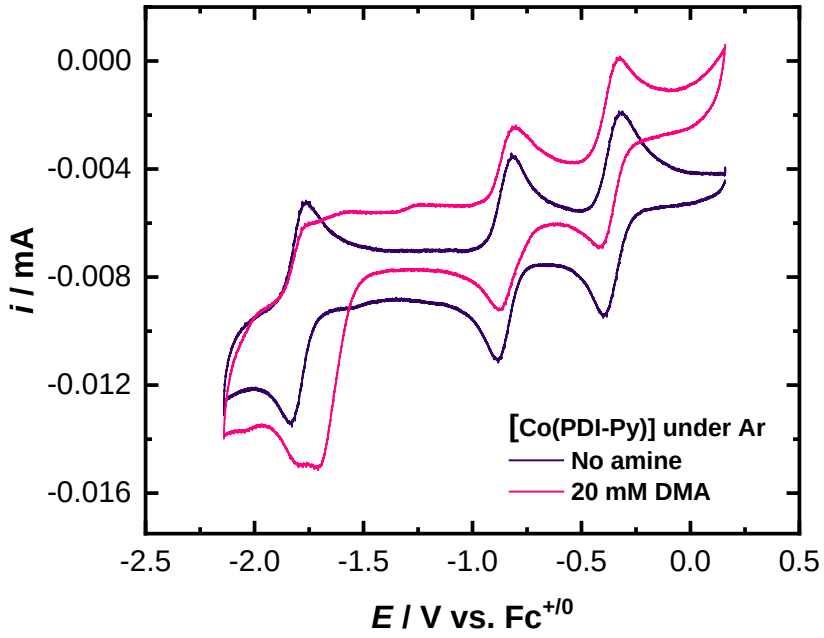

Figure S13. Representative CVs of 0.3 mM [Co(PDI-Py)] in Ar-sparged MeCN with 0.1 M *n*Bu$_4$NPF$_6$ at a scan rate of 0.05 V/s with and without 20.0 mM DMA.

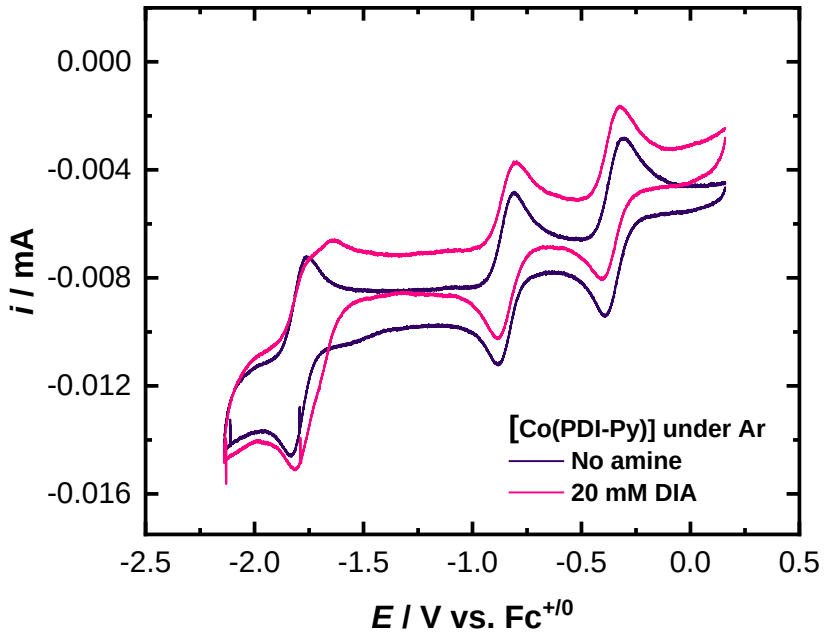

Figure S14. Representative CVs of 0.3 mM [Co(PDI-Py)] in Ar-sparged MeCN with 0.1 M *n*Bu$_4$NPF$_6$ at a scan rate of 0.05 V/s with and without 20.0 mM DIA.

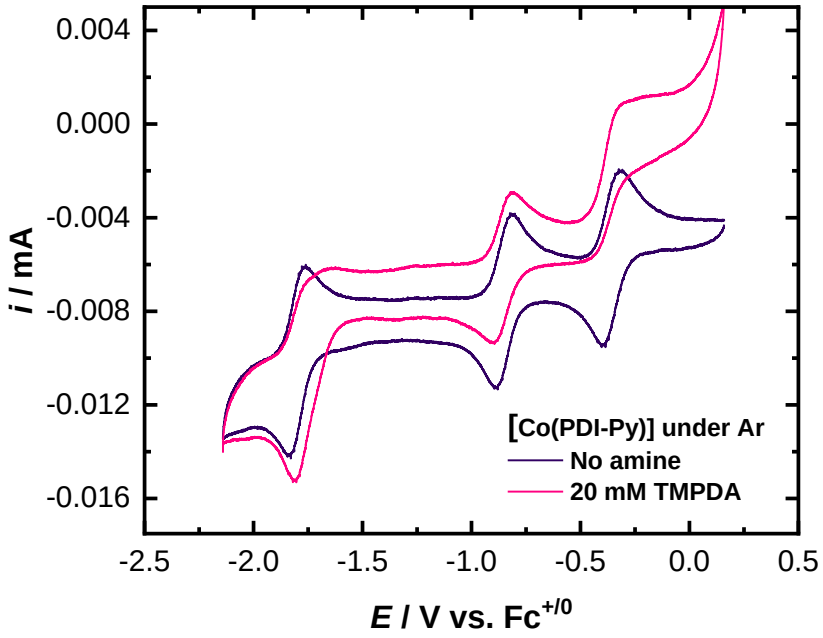

Figure S15. Representative CVs of 0.3 mM [Co(PDI-Py)] in Ar-sparged MeCN with 0.1 M nBu$_4$NPF$_6$ at a scan rate of 0.05 V/s with and without 20.0 mM TMPDA

Table S2: $E_{1/2}$ values of the $Co^{3+/2+}$ and $Co^{2+/+}$ redox couples for [Co(PDI-Py)], Ar-sparged MeCN with 0.1 M nBu$_4$PF$_6$.

	$Co^{3+/2+}$ / V vs $Fc^{+/0}$	$Co^{2+/+}$ / V vs $Fc^{+/0}$
No amine	-0.36	-0.86
NBA	-0.42	-0.86
MEA	-0.39	-0.85
DMA	-0.37	-0.84
DIA	-0.36	-0.84
TPDA	-0.38	-0.85

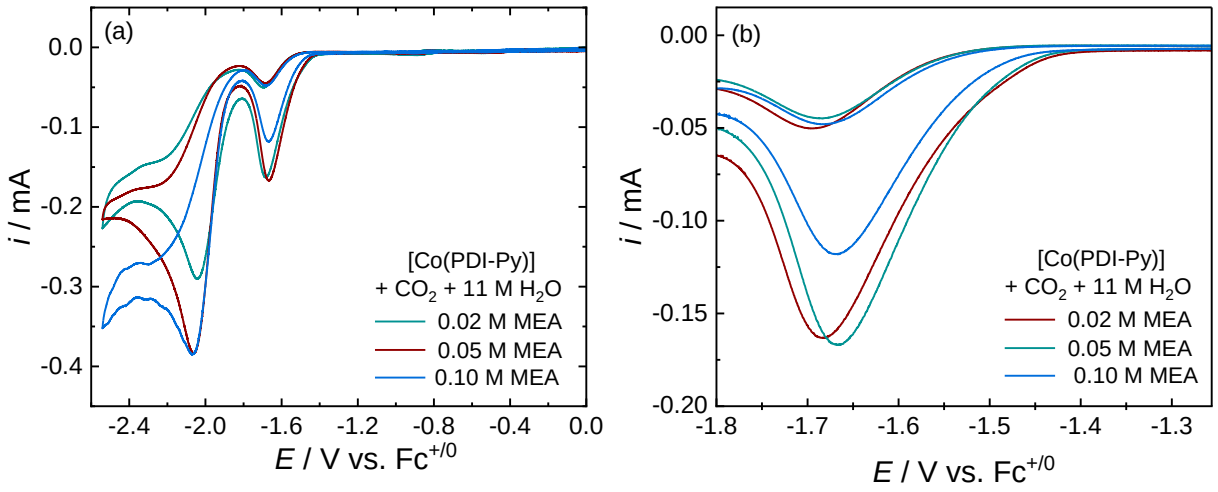

Figure S16. (a) Representative CVs of 0.3 mM [Co(PDI-Py)] in CO_2-sparged MeCN with 0.1 M nBu$_4$NPF$_6$ and 11 M H_2O at a scan rate of 50 mV/s with different concentrations of MEA; (b) zoomed-in view of the CO_2 reduction peak at ~−1.65 V vs $Fc^{+/0}$.

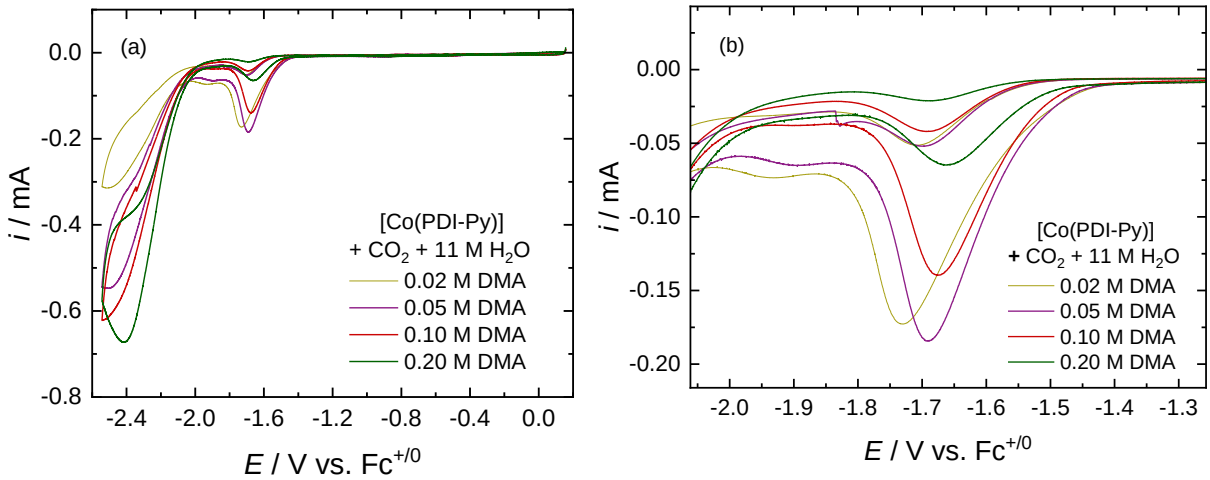

Figure S17. (a) Representative CVs of 0.3 mM [Co(PDI-Py)] in CO_2-sparged MeCN with 0.1 M nBu$_4$NPF$_6$ and 11 M H_2O at a scan rate of 50 mV/s with different concentrations of DMA; (b) zoomed-in view of the CO_2 reduction peak at ~−1.65 V vs $Fc^{+/0}$.

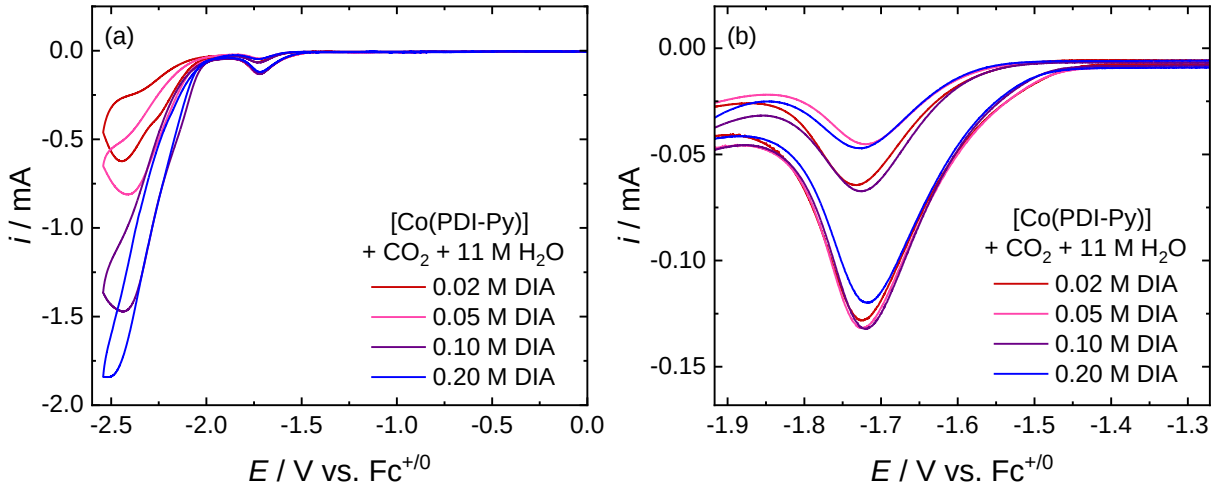

Figure S18. (a) Representative CVs of 0.3 mM [Co(PDI-Py)] in CO_2-sparged MeCN with 0.1 M nBu$_4$NPF$_6$ and 11 M H_2O at a scan rate of 50 mV/s with different concentrations of DIA; (b) zoomed-in view of the CO_2 reduction peak at ~−1.65 V vs $Fc^{+/0}$.

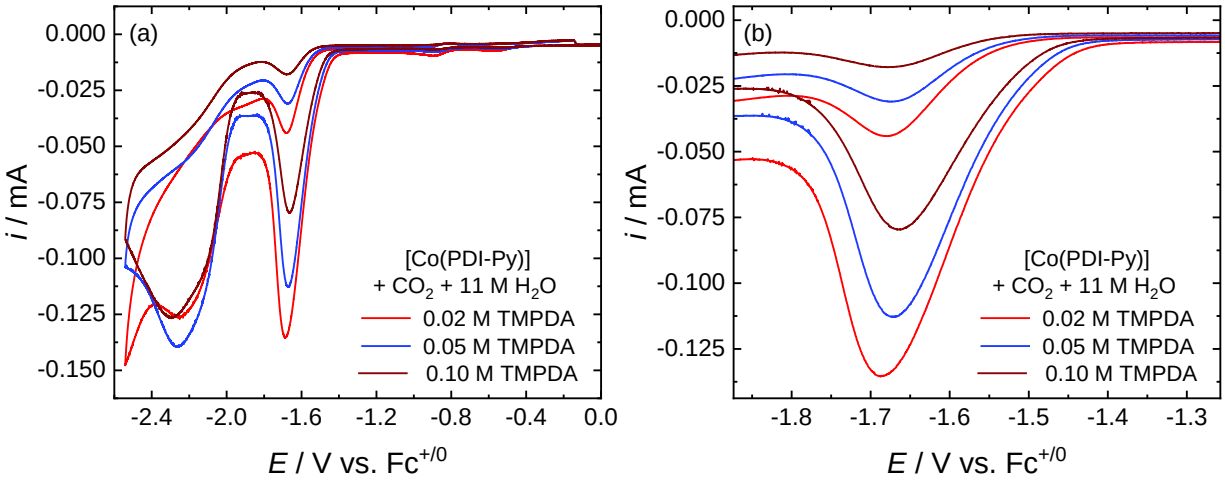

Figure S19. (a) Representative CVs of 0.3 mM [Co(PDI-Py)] in CO_2-sparged MeCN with 0.1 M nBu$_4$NPF$_6$ and 11 M H_2O at a scan rate of 50 mV/s with different concentrations of TMPDA; (b) zoomed-in view of the CO_2 reduction peak at ~−1.65 V vs $Fc^{+/0}$.

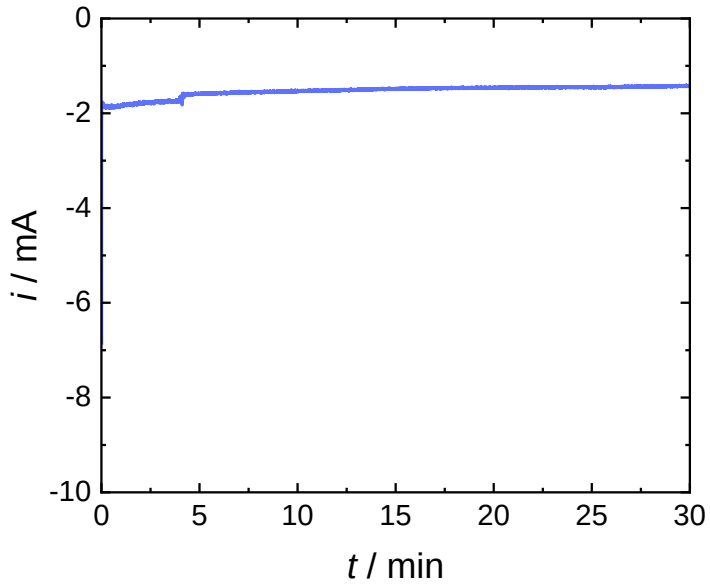

Figure S20. Representative 30 min CPE current trace of the CO_2RR by [Co(PDI-Py)] in CO_2-sparged MeCN with 0.1 M nBu$_4$NPF$_6$ and 11 M H_2O with no amine present at −1.69 V vs $Fc^{+/0}$.

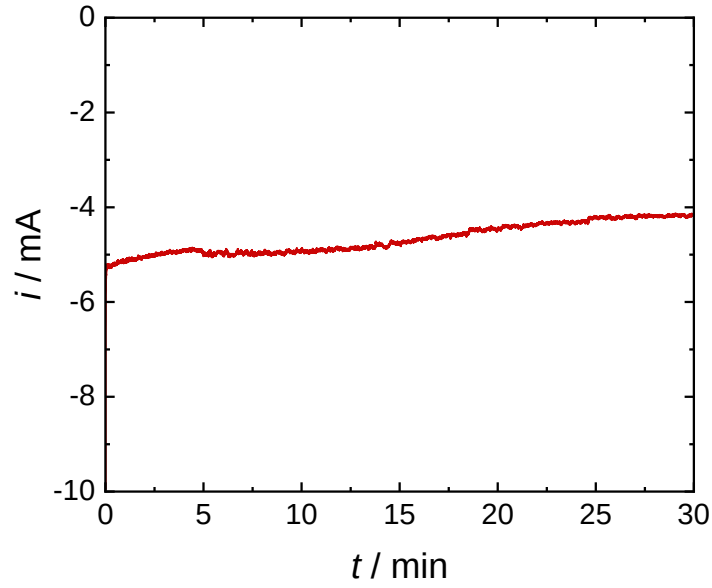

Figure S21. Representative 30 min CPE current trace of the CO_2RR by [Co(PDI-Py)] in CO_2-sparged MeCN with 0.1 M nBu$_4$NPF$_6$ and 11 M H_2O with 0.05 M NBA at −1.69 V vs $Fc^{+/0}$.

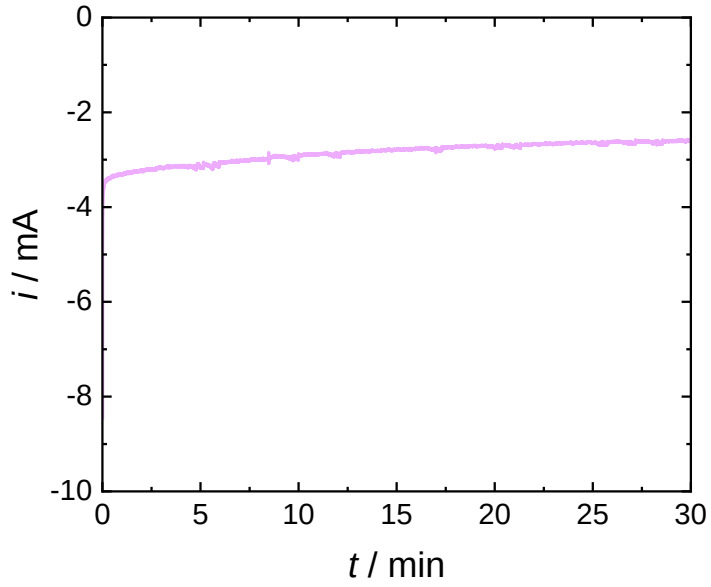

Figure S22. Representative 30 min CPE current trace of the CO_2RR by [Co(PDI-Py)] in CO_2-sparged MeCN with 0.1 M nBu$_4$NPF$_6$ and 11 M H_2O with 0.05 M MEA at −1.69 V vs $Fc^{+/0}$.

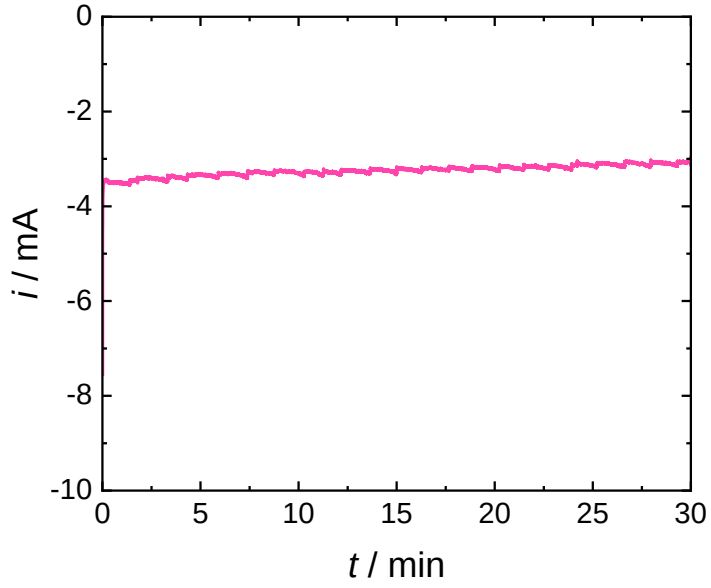

Figure S23. Representative 30 min CPE current trace of the CO_2RR by [Co(PDI-Py)] in CO_2-sparged MeCN with 0.1 M nBu$_4$NPF$_6$ and 11 M H_2O with 0.05 M DMA at −1.69 V vs $Fc^{+/0}$.

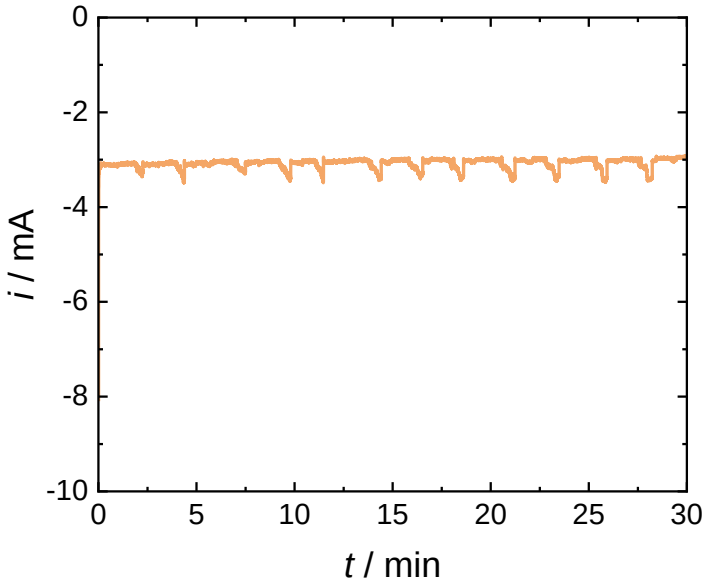

Figure S24. Representative 30 min CPE current trace of the CO_2RR by [Co(PDI-Py)] in CO_2-sparged MeCN with 0.1 M nBu$_4$NPF$_6$ and 11 M H_2O with 0.05 M DIA at −1.69 V vs $Fc^{+/0}$.

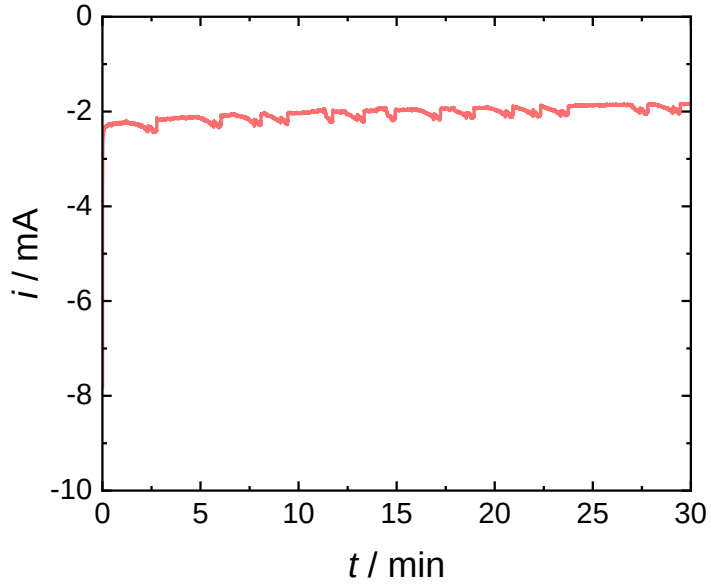

Figure S25. Representative 30 min CPE current trace of the CO_2RR by [Co(PDI-Py)] in CO_2-sparged MeCN with 0.1 M nBu$_4$NPF$_6$ and 11 M H_2O with 0.05 M TMPDA at −1.69 V vs $Fc^{+/0}$.

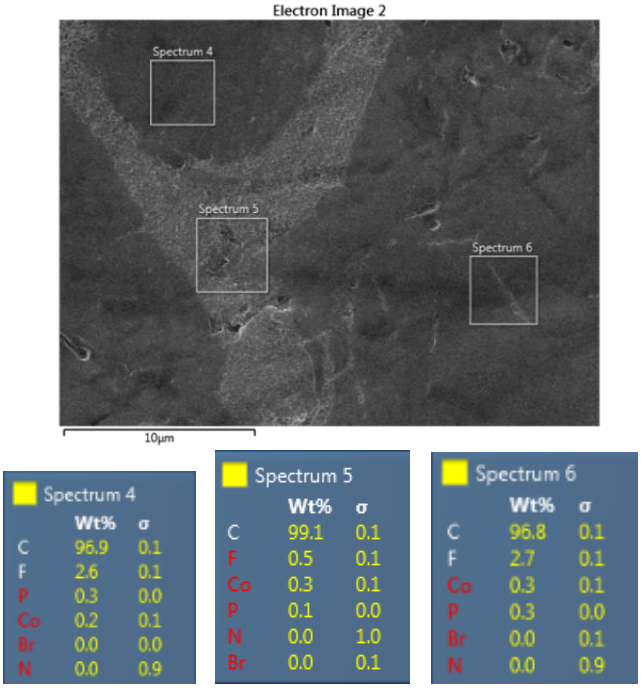

Figure S26. SEM-EDS analysis of the glassy carbon working electrode surface after 30 min CO_2RR electrolysis of 0.3mM [Co(PDI-Py)] CO_2-saturated MeCN with 0.1 M nBu$_4$NPF$_6$ and 11 M H_2O (without amine) at -1.69 V vs $Fc^{+/0}$.

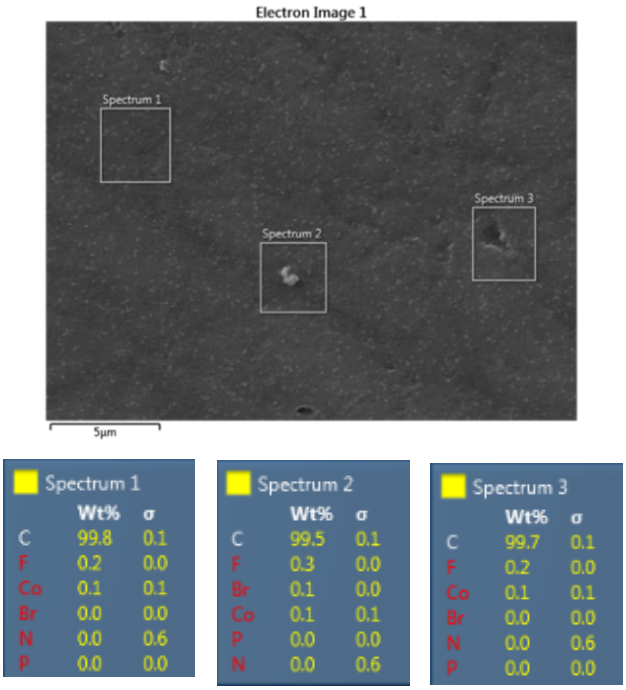

Figure S27. SEM-EDS analysis of the glassy carbon working electrode surface after 30 min CO_2RR electrolysis of 0.3mM [Co(PDI-Py)] CO_2-saturated MeCN with 0.1 M nBu$_4$NPF$_6$ and 11 M H_2O and 0.05 M NBA at -1.69 V vs $Fc^{+/0}$.

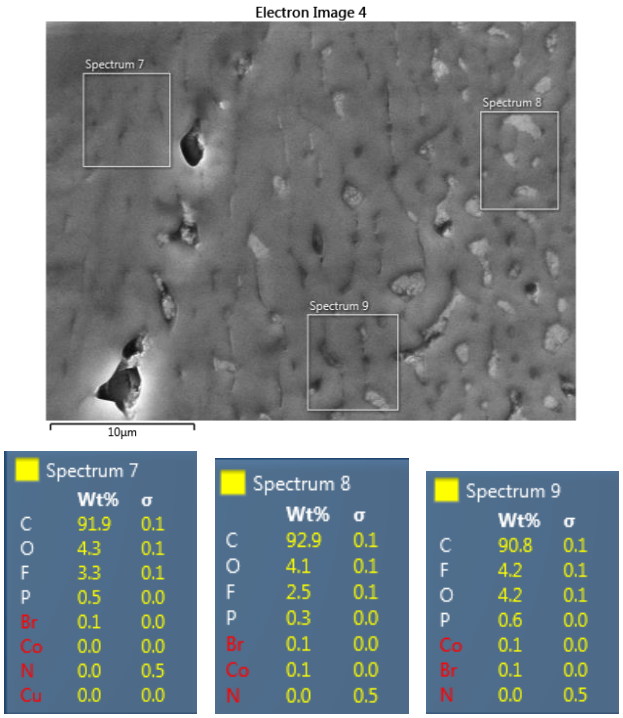

Figure S28. SEM-EDS analysis of the glassy carbon working electrode surface after 30 min CO_2RR electrolysis of 0.3mM [Co(PDI-Py)] CO_2-saturated MeCN with 0.1 M nBu$_4$NPF$_6$ and 11 M H_2O and 0.05 M MEA at -1.69 V vs $Fc^{+/0}$.

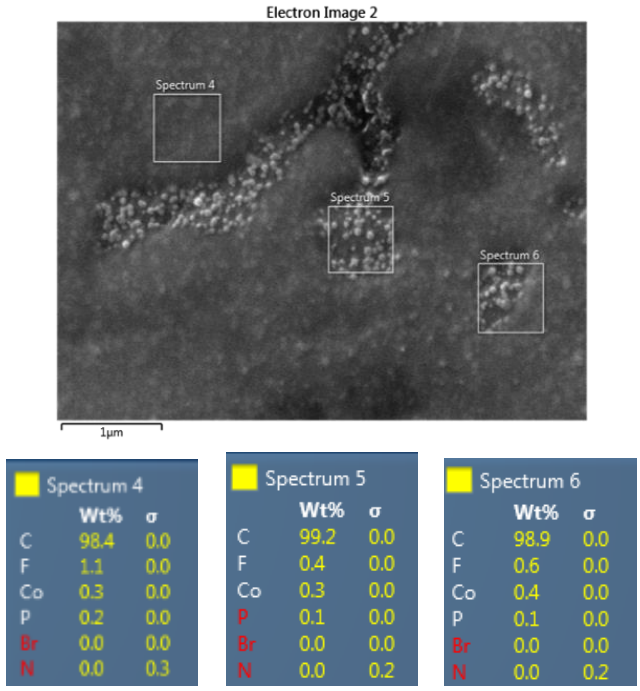

Figure S29. SEM-EDS analysis of the glassy carbon working electrode surface after 30 min CO_2RR electrolysis of 0.3mM [Co(PDI-Py)] CO_2-saturated MeCN with 0.1 M nBu$_4$NPF$_6$ and 11 M H_2O and 0.05 M DIA at -1.69 V vs $Fc^{+/0}$.

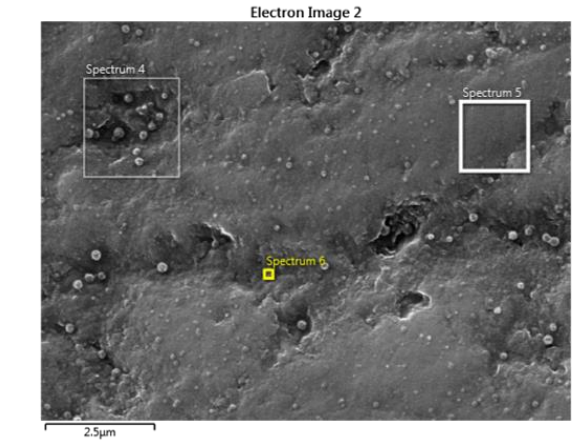

Spectrum 4	Wt%	σ
C	92.2	0.1
O	7.6	0.0
Co	0.1	0.0
Br	0.0	0.0
P	0.0	0.0
N	0.0	0.2
F	0.0	0.0

Spectrum 5	Wt%	σ
C	92.1	0.0
O	7.8	0.0
Br	0.0	0.0
Co	0.0	0.0
P	0.0	0.0
N	0.0	0.2
F	0.0	0.0

Spectrum 6	Wt%	σ
C	89.1	0.1
O	10.2	0.1
Co	0.5	0.0
Br	0.2	0.0
F	0.0	0.0
P	0.0	0.0
N	0.0	0.3

Figure S30. SEM-EDS analysis of the glassy carbon working electrode surface after 30 min CO_2RR electrolysis of 0.3mM [Co(PDI-Py)] CO_2-saturated MeCN with 0.1 M nBu$_4$NPF$_6$ and 11 M H_2O and 0.05 M DMA at -1.69 V vs $Fc^{+/0}$.

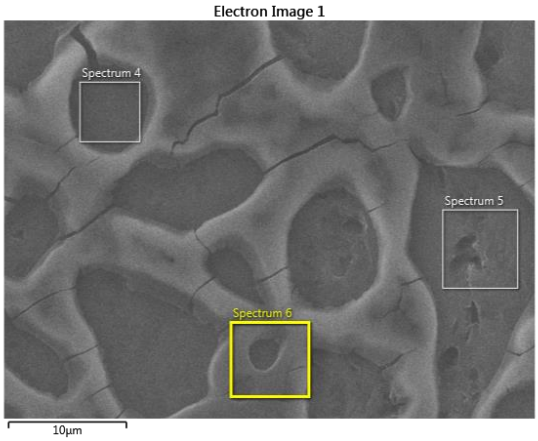

Spectrum 4	Wt%	σ
C	98.9	0.2
F	0.9	0.1
Co	0.1	0.1
P	0.1	0.0
Br	0.0	0.1
N	0.0	1.4

Spectrum 5	Wt%	σ
C	99.4	0.1
F	0.5	0.1
P	0.0	0.0
Br	0.0	0.1
N	0.0	1.3
Co	0.0	0.1

Spectrum 6	Wt%	σ
C	87.2	1.2
F	11.7	1.2
P	1.0	0.3
N	0.0	5.7
Br	0.0	0.3
Co	0.0	0.4

Figure S31. SEM-EDS analysis of the glassy carbon working electrode surface after 30 min CO_2RR electrolysis of 0.3mM [Co(PDI-Py)] CO_2-saturated MeCN with 0.1 M nBu$_4$NPF$_6$ and 11 M H_2O and 0.05 M TMPDA at -1.69 V vs $Fc^{+/0}$.

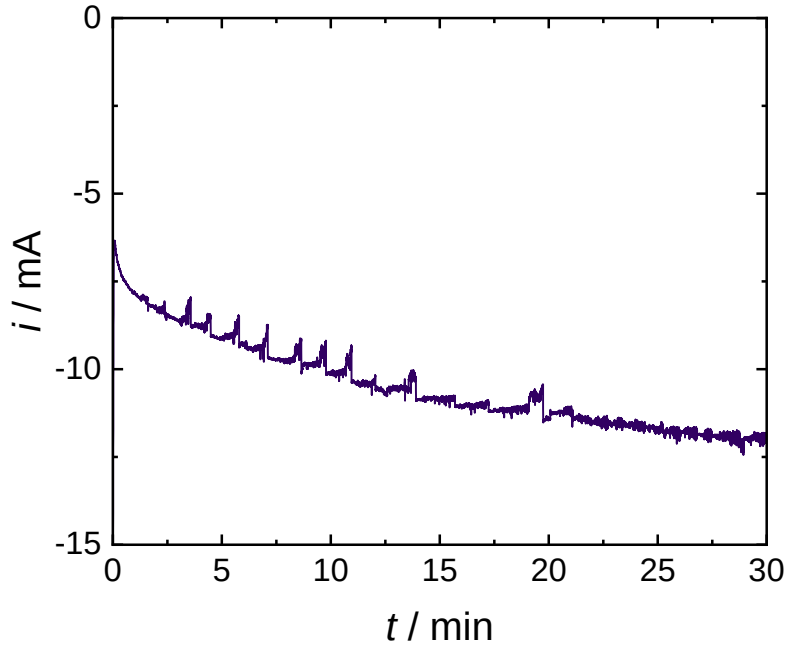

Figure S32. Representative 30 min CPE current trace of [Co(PDI-Py)] in CO_2-sparged MeCN with 0.1 M nBu$_4$NPF$_6$ and 11 M H_2O with 0.05 M NBA at −2.34 V vs $Fc^{+/0}$.

Table S3: Summary of the experimental results for 30-min CPEs of the CO_2RR by [Co(PDI-Py)] in CO_2-saturated solution containing 0.3 mM [Co(PDI-Py)], 0.1 M nBuNPF$_6$, 11 M H_2O, and 0.05 M NBA at −2.34 V vs $Fc^{+/0}$.

Charge / C	FE (H_2) /%	FE (CO) /%
18.8	83.6	11.5

Table S4: Summary of the experimental results for 30-min CPEs of the reduction of DMA-CO_2 by [Co(PDI-Py)] in N_2-saturated solution containing 0.3 mM [Co(PDI-Py)], 0.1 M nBuNPF$_6$, 11 M H_2O, and 0.05 M DMA-CO_2 at −1.69 V vs $Fc^{+/0}$.

Charge / C	FE (CO) /%	FE (H_2) /%
1.9 ± 0.5	16.2 ± 2.8	5.6 ± 0.9

Very little charge was passed during the electrolysis of DMA-CO_2 with [Co(PDI-Py)]. Up to 0.579 C of charge (~30%) can be attributed to the reduction of 0.3 mM [Co(PDI-Py)Br$_2$]Br to [Co(PDI-Py)Br$_2$] to enter the catalytic cycle. Only ~21.8% of the charge can be accounted for by measured products, meaning ~50% of the charge is unaccounted for.

Control CPEs of bare glassy carbon plates in Ar-sparged electrolyte with no catalyst or amine under otherwise identical conditions passed virtually no charge (0.07 C). However, control CPEs of bare glassy carbon plates in Ar-sparged electrolyte with 0.05 M DMA-CO_2 passed 1.3 C with no measured CO and 13% H_2 production.

These experimental results suggest that in the CPEs of DMA-CO_2 with [Co(PDI-Py)] present, the unaccounted for charge is likely going to some side reaction of the carbamate species for which the products could not be identified via GC or NMR measurements.

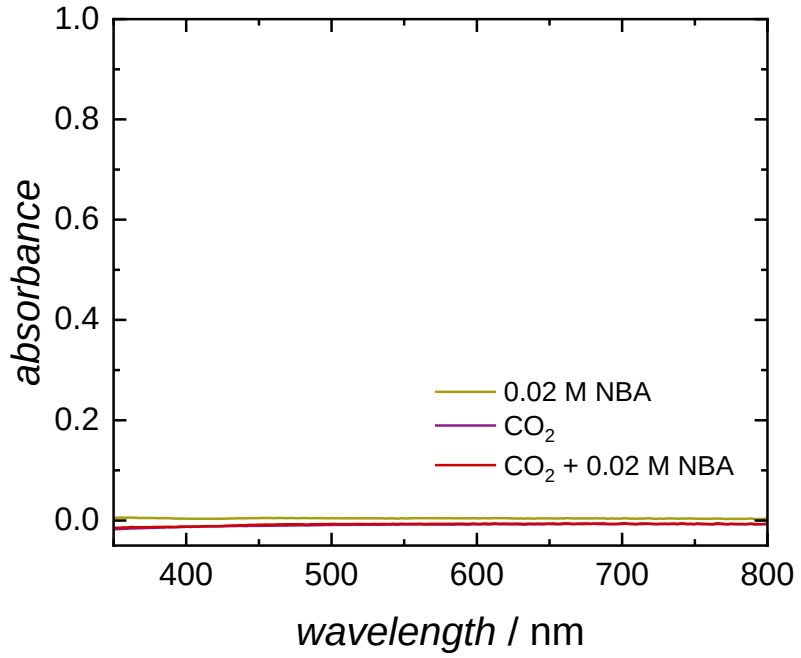

Figure S33. UV-Vis spectra of solutions containing NBA, CO_2, and both CO_2 and NBA in MeCN with 0.1 M nBu$_4$NPF$_6$ and 11 M H_2O solution in MeCN.

Samples for UV-Vis experiments were prepared using solutions of 0.02 M of NBA in 0.1 M of nBu$_4$NPF$_6$ and 11 M H_2O in MeCN as follows:

Experiment (a): The 0.02 M of NBA solution was sparged with N_2 for 20 min prior to collecting a UV-Vis spectrum.

Experiment (b): The electrolyte solution (0.1 M of nBu$_4$NPF$_6$ and 11 M H_2O in MeCN) without NBA was sparged with CO_2 for 10 min and a UV-Vis spectrum was recorded.

Experiment (c): 0.02 M of NBA solution was sparged with CO_2 for 10 min, and UV-Vis spectrum of the resulting dilute solution was recorded.

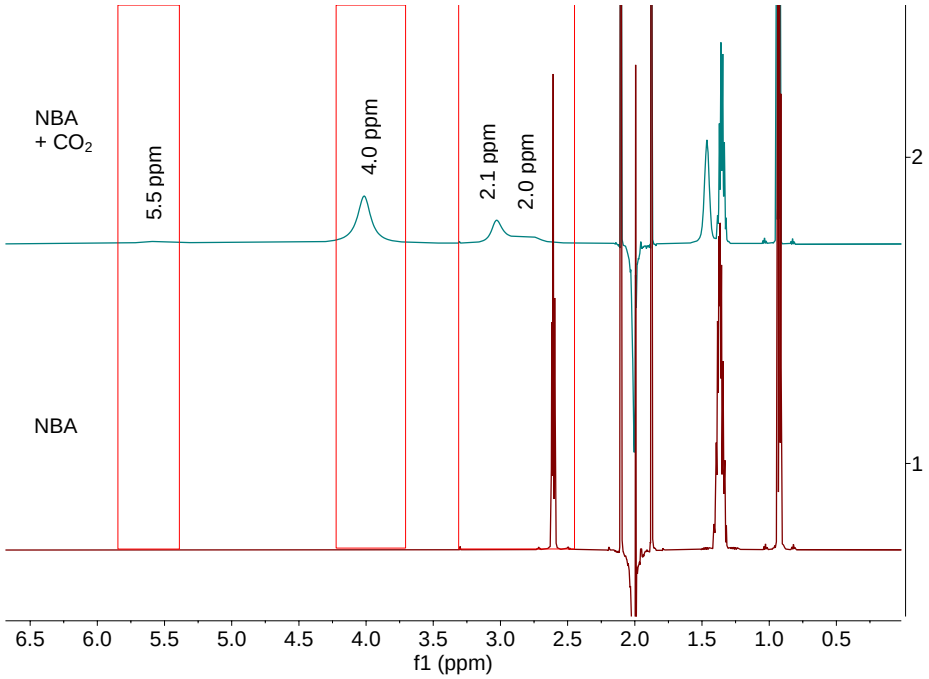

Figure S34. ^{1}H NMR spectra of (top) 0.05 M NBA in Ar-sparged MeCN, and (bottom) 0.05 M NBA in CO_2-sparged MeCN. Solvent peak for MeCN at δ 1.9 ppm was suppressed by single solvent suppression method.

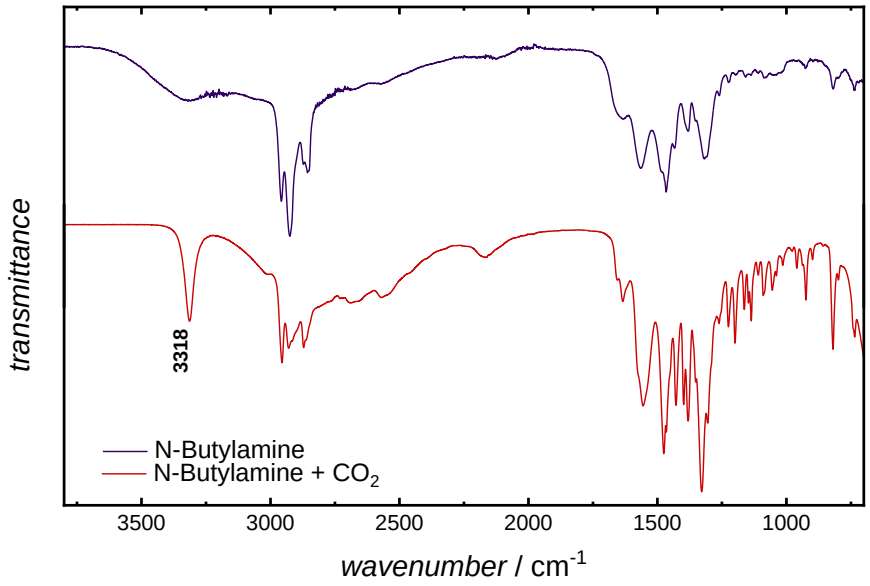

Figure S35. FT-IR of NBA (blue trace) and the solid product obtained upon reacting NBA with CO_2 (red trace). The peak at 3318 cm^{-1} is an O-H stretching frequency consistent with the formation of *n*-butylcarbamic acid.

References:

S1. D. B. G. Williams and M. Lawton, *J. Org. Chem.*, 2010, **75**, 8351-8354.

S2. Y. Hui and R. D. Webster, *Anal. Chem.*, 2011, **83**, 976-981.

S3. C. C. L. McCrory, N. K. Szymczak and J. C. Peters, *Electrocatalysis*, 2016, **7**, 87-96.

S4. W. Nie, D. E. Tarnopol and C. C. L. McCrory, *J. Am. Chem. Soc.*, 2021, **143**, 3764-3778.

S5. W. Nie, Y. Wang, T. Zheng, A. Ibrahim, Z. Xu and C. C. L. McCrory, *ACS Catal.*, 2020, **10**, 4942-4959.

S6. W. Nie and C. C. L. McCrory, *Chem. Commun.*, 2018, **54**, 1579-1582.